

# Synergistic Regulation of Glutamatergic Transmission by Serotonin and Norepinephrine Reuptake Inhibitors in Prefrontal Cortical Neurons\*

Received for publication, March 21, 2014, and in revised form, July 7, 2014. Published, JBC Papers in Press, July 23, 2014, DOI 10.1074/jbc.M114.567610

Eunice Y. Yuen<sup>‡</sup>, Luye Qin<sup>‡</sup>, Jing Wei<sup>‡§</sup>, Wenhua Liu<sup>‡</sup>, Aiyi Liu<sup>‡</sup>, and Zhen Yan<sup>‡§1</sup>

From the <sup>‡</sup>Department of Physiology and Biophysics, School of Medicine and Biomedical Sciences, State University of New York, Buffalo, New York 14214 and <sup>§</sup>Veterans Affairs Western New York Healthcare System, Buffalo, New York 14215

**Background:** Serotonin and norepinephrine reuptake inhibitors (SNRIs) produce better therapeutic effects than single selective reuptake inhibitors, but the underlying mechanisms are largely unknown.

**Results:** Low dose SNRIs, by acting on 5-HT<sub>1A</sub> and  $\alpha_2$ -AR, synergistically reduced glutamatergic transmission in prefrontal cortex (PFC).

**Conclusion:** SNRIs exerts a powerful impact on PFC synaptic activity.

**Significance:** Our study provides a mechanism for the therapeutic effects of SNRIs in mental disorders related to PFC dysfunction.

The monoamine system in the prefrontal cortex has been implicated in various mental disorders and has been the major target of anxiolytics and antidepressants. Clinical studies show that serotonin and norepinephrine reuptake inhibitors (SNRIs) produce better therapeutic effects than single selective reuptake inhibitors, but the underlying mechanisms are largely unknown. Here, we found that low dose SNRIs, by acting on 5-HT<sub>1A</sub> and  $\alpha_2$ -adrenergic receptors, synergistically reduced AMPA receptor (AMPA)-mediated excitatory postsynaptic currents and AMPAR surface expression in prefrontal cortex pyramidal neurons via a mechanism involving Rab5/dynamin-mediated endocytosis of AMPARs. The synergistic effect of SNRIs on AMPARs was blocked by inhibition of activator of G protein signaling 3, a G protein modulator that prevents reassociation of G<sub>i</sub> protein  $\alpha$  subunit and prolongs the  $\beta\gamma$ -mediated signaling pathway. Moreover, the depression of AMPAR-mediated excitatory postsynaptic currents by SNRIs required p38 kinase activity, which was increased by 5-HT<sub>1A</sub> and  $\alpha_2$ -adrenergic receptor co-activation in an activator of G protein signaling 3-dependent manner. These results have revealed a potential mechanism for the synergy between the serotonin and norepinephrine systems in the regulation of glutamatergic transmission in cortical neurons.

Monoamines, such as serotonin (5-HT)<sup>2</sup> and norepinephrine (NE), play important roles in cognitive and emotional pro-

cesses mediated by the prefrontal cortex (PFC) (1, 2). Changing 5-HT and NE transmission has been the core mechanism among antidepressants and anxiolytics (3–7). Because monoamines do not pass the blood-brain barrier, effective drugs act as reuptake inhibitors to raise their synaptic concentrations. Clinical trials suggest that drugs increasing both 5-HT and NE levels at synapses give more robust therapeutic effects than those increasing a single neurotransmitter alone, including faster onset of therapeutic effects and lower relapse rate (4, 8, 9). However, little is known about the underlying mechanisms.

Both serotonin receptors and adrenergic receptors have multiple subtypes that can be grouped into different classes based on their pharmacological and signaling properties (10, 11). Among these receptors, 5-HT<sub>1A</sub> and  $\alpha_2$ -AR are G<sub>i</sub>-coupled G protein-coupled receptors enriched in dendritic spines (12, 13) where glutamatergic transmission occurs. Abnormal expression and signaling mediated by 5-HT<sub>1A</sub> and  $\alpha_2$ -AR have been highly implicated in psychiatric disorders. For example, genetic knock-out of 5-HT<sub>1A</sub> or  $\alpha_2$ -AR leads to an elevated anxiety phenotype (14, 15). Post-mortem brains of depressed patients show altered receptor levels or ligand binding (16, 17). The 5-HT<sub>1A</sub> and  $\alpha_2$ -AR gene polymorphisms or altered receptor functions correlate well with the prevalence of depression in humans (18) as well as the effectiveness of antidepressants (19, 20).

In the present study, we identified that AMPAR is the cellular target of monoamines in the prefrontal cortex. A low dose of serotonin and norepinephrine reuptake inhibitors (SNRIs), by simultaneously activating 5-HT<sub>1A</sub> and  $\alpha_2$ -AR, synergistically suppressed glutamatergic transmission in PFC pyramidal neurons through a mechanism involving AMPAR internalization. Given the significance of AMPAR-mediated excitation in PFC-dependent functions (21, 22), our results provide a potential basis for the better effects of dual reuptake inhibitors in therapeutic intervention of mental disorders related to PFC dysfunction.

\* This work was supported, in whole or in part, by National Institutes of Health Grants MH101690 and DA037618 (to Z. Y.). This work was also supported by Veterans Affairs Merit Award 1101BX001633 (to Z. Y.).

<sup>1</sup> To whom correspondence should be addressed: Dept. of Physiology and Biophysics, State University of New York, 124 Sherman Hall, Buffalo, NY 14214. E-mail: zhenyan@buffalo.edu.

<sup>2</sup> The abbreviations used are: 5-HT, serotonin (5-hydroxytryptamine); NE, norepinephrine; SNRI, serotonin and norepinephrine reuptake inhibitor; PFC, prefrontal cortex; EPSC, excitatory postsynaptic current; AMPAR, AMPA receptor; AR, adrenergic receptor; AGS3, activator of G protein signaling 3; AMPAR-EPSC, AMPAR-mediated EPSC; mEPSC, miniature EPSC; 8-OH-DPAT, 8-hydroxy-2-(di-*n*-propylamino)tetralin; GluR, glutamate receptor; ANOVA, analysis of variance.

### EXPERIMENTAL PROCEDURES

**Electrophysiological Recordings in Slices and Cultures**—The whole-cell voltage clamp technique was used to record AMPAR-mediated excitatory postsynaptic current (AMPA-EPSC) in PFC layer V pyramidal neurons from postnatal rats (3–4 weeks) as we described previously (23–25). Slices (300  $\mu\text{m}$ ) were perfused with artificial cerebrospinal fluid bubbled with 95%  $\text{O}_2$  and 5%  $\text{CO}_2$  containing D-2-amino-5-phosphonovalerate (25  $\mu\text{M}$ ) and bicuculline (10  $\mu\text{M}$ ). The internal solution contained 130 mM cesium methanesulfonate, 10 mM CsCl, 4 mM NaCl, 1 mM  $\text{MgCl}_2$ , 10 mM HEPES, 5 mM EGTA, 2.2 mM QX-314, 12 mM phosphocreatine, 5 mM MgATP, and 0.5 mM  $\text{Na}_2\text{GTP}$ , pH 7.2–7.3, 265–270 mosM. Neurons were visualized with a 40 $\times$  water immersion lens and illuminated with near infrared (IR) light. All recordings were performed using a Multiclamp 700A amplifier with neurons held at  $-70$  mV. Tight seals (2–10 gigaohms) were generated by applying negative pressure followed by additional suction to disrupt the membrane and obtain the whole-cell configuration. EPSCs were stimulated by exciting the neighboring cortical neurons with a bipolar tungsten electrode (FHC, Inc.) located at a few hundred micrometers away from the neuron under recording.

Rat cortical cultures were prepared by modified methods as described previously (24, 26). After treatment or transfection, the miniature EPSC (mEPSC) recordings in culture neurons (21–24 days *in vitro*) were performed in the presence of D-2-amino-5-phosphonovalerate (25  $\mu\text{M}$ ), bicuculline (10  $\mu\text{M}$ ), and tetrodotoxin (1  $\mu\text{M}$ ).

The agents we used include fluoxetine, 8-hydroxy-2-(di-*n*-propylamino)tetralin (8-OH-DPAT), WAY-100635 (Sigma), desipramine, venlafaxine, clonidine hydrochloride, yohimbine hydrochloride, SB203480, PD98059, and dynamin inhibitory peptide (Tocris). They were made up as concentrated stocks in water or DMSO and stored at  $-20$  °C. Stocks were thawed and diluted immediately prior to experiments.

**Biochemical Measurement of Surface Receptors**—The surface AMPA receptors were detected as described previously (23, 24). After treatment, PFC slices were incubated in PBS containing 1 mg/ml Sulfo-NHS-LC-Biotin (Pierce) on ice for 40 min. The slices were then rinsed three times in TBS to quench the biotin reaction followed by homogenization in 500  $\mu\text{l}$  of modified radioimmune precipitation assay buffer containing 1% Triton X-100, 0.1% SDS, 0.5% deoxycholic acid, 50 mM  $\text{NaPO}_4$ , 150 mM NaCl, 2 mM EDTA, 50 mM NaF, 10 mM sodium pyrophosphate, 1 mM sodium orthovanadate, 1 mM PMSF, and 1 mg/ml leupeptin. The homogenates were centrifuged at  $16,000 \times g$  for 30 min at 4 °C. The supernatant was collected and incubated with NeutrAvidin-agarose (Pierce) for 2 h at 4 °C. Bound proteins were washed three times with radioimmune precipitation assay buffer and subjected to SDS-PAGE. Western blotting was performed on biotinylated (surface) and total proteins using antibodies against GluR1 or GluR2 (both at 1:500; Chemicon).

**Immunocytochemistry**—After transfection and treatment, neurons were fixed in 4% paraformaldehyde in PBS for 20 min at room temperature and incubated with 5% bovine serum albumin (BSA) for 1 h to block nonspecific staining. Cells were

then permeabilized with 0.2% Triton X-100 for 20 min at room temperature followed by incubation with the primary antibody at 4 °C overnight. For measuring the levels of total and active p38 MAPK, anti-p38 and anti-<sup>Thr-180/Tyr-182</sup>phospho-p38 antibodies (1: 500; Cell Signaling Technology) were used. After washing, neurons were incubated with Alexa Fluor 488 (green)- or Alexa Fluor 594 (red)-conjugated secondary antibodies (1:500; Molecular Probes) for 2 h at room temperature. After washing in PBS three times, the coverslips were mounted on slides with VECTASHIELD mounting medium (Vector Laboratories, Burlingame, CA). Images were captured with identical conditions and analyzed with identical parameters. The intensity of p38 signal was quantified using NIH ImageJ software.

**Small Interfering RNA**—To knock down endogenous activator of G protein signaling 3 (AGS3) expression, we used the small interfering RNA (siRNA) specifically targeting AGS3 (Santa Cruz Biotechnology, Santa Cruz, CA): 5'-CGAGAGCACUCUACAACAU-3', 5'-GCUGAACAUUACAAGAAGA-3', and 5'-CCAAGCAUAGGGUCUUGUA-3'. AGS3 siRNA oligos were co-transfected with enhanced GFP into cultured PFC neurons (21 days *in vitro*) using the Lipofectamine 2000 method. A scrambled siRNA was used as control. Western blot analysis of AGS3 expression was performed to validate the gene silencing efficiency of AGS3 siRNA using anti-AGS3 antibody (1:500; Santa Cruz Biotechnology). Biochemical, immunocytochemical, or electrophysiological experiments were performed after 2–3 days of transfection.

**Cloning, Expression, and Purification of Proteins**—Purified Rab5 protein was generated using a method similar to that described previously (27). Using mouse brain total RNA, wild-type Rab5 cDNA was cloned by RT-PCR followed by sequence verification. The cDNA was then subcloned into the bacterial expression vector pQE-80 (Qiagen, Valencia, CA), which added a His<sub>6</sub> tag at the N terminus of the protein. Rab5 mutants (S34N and Q79L) were generated by site-directed mutagenesis using the QuikChange kit from Stratagene (La Jolla, CA). Rab5 expression in the M15 strain of *Escherichia coli* (Qiagen) was induced by adding isopropyl  $\beta$ -D-thiogalactoside to 1 mM final concentration for 4–5 h at 25 °C (to minimize the formation of inclusion bodies). Rab5 in cleared *E. coli* lysate was purified by affinity chromatography using a His Gravitrap column (GE Healthcare) according to the manufacturer's protocol. His<sub>6</sub>-tagged Rab5 proteins were eluted from the column in a buffer containing 50 mM Tris, 500 mM NaCl, and 300 mM imidazole, pH 7.4. Fractions of eluate were analyzed by SDS-polyacrylamide gel electrophoresis and Coomassie Blue staining to identify the peak fractions containing Rab5 proteins. Western blotting with the polyclonal anti-Rab5 (Santa Cruz Biotechnology) was also performed to verify the expression of purified Rab5 protein. One to two of the most pure fractions (shown as a single band by Coomassie Blue staining) were dialyzed against phosphate-buffered saline before being used in electrophysiological experiments.

**Statistics**—Data analyses were performed with AxoGraph (Axon Instruments), Kaleidagraph (Albeck Software, Reading, PA), Origin 6 (Microcal Software, Northampton, MA), and Statview (Abacus Concepts, Calabasas, CA). All data are

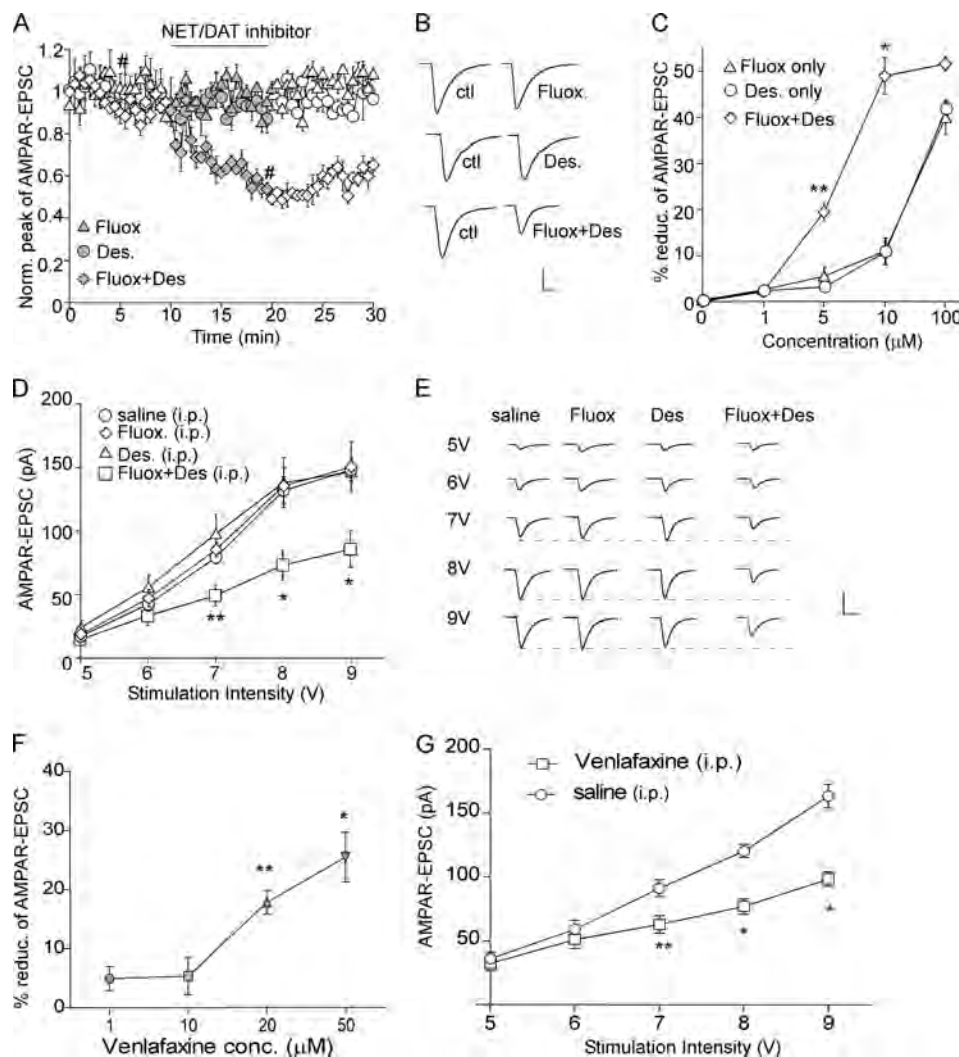


**FIGURE 1. SNRIs produce a synergistic reduction of AMPAR-EPSC in PFC pyramidal neurons.** *A*, plot of normalized (*Norm.*) peak AMPAR-EPSC recorded in PFC slices treated with the selective 5-HT reuptake inhibitor fluoxetine alone (10  $\mu\text{M}$ ), the selective NE reuptake inhibitor desipramine alone (10  $\mu\text{M}$ ), or both. *B*, representative current traces taken at the time points denoted by # in *A*. Scale bar, 50 pA, 10 ms. *C*, dose-response plot showing the percentage of reduction of EPSC by single or dual application of fluoxetine and desipramine at various concentrations. \*,  $p < 0.01$ ; \*\*,  $p < 0.05$ , two-way ANOVA. *D*, input-output curve of AMPAR-EPSC amplitude evoked by different stimulation intensities in PFC slices taken from animals injected (intraperitoneally) without or with fluoxetine (5 mg/kg), desipramine (1 mg/kg), or both. \*,  $p < 0.01$ ; \*\*,  $p < 0.05$ , two-way ANOVA. *E*, representative EPSC traces in animals injected with different inhibitors. Scale bar, 100 pA, 20 ms. *F*, dose-response plot showing the percentage of reduction (*reduc.*) of AMPAR-EPSC by application of venlafaxine at various concentrations. \*,  $p < 0.01$ ; \*\*,  $p < 0.05$ , one-way ANOVA. *G*, input-output curve of AMPAR-EPSC amplitude evoked by different stimulation intensities in PFC slices taken from animals injected with saline or venlafaxine (8 mg/kg; intraperitoneally). \*,  $p < 0.01$ ; \*\*,  $p < 0.05$ , two-way ANOVA. Error bars represent S.E. *ctl*, control; *Fluox*, fluoxetine; *Des*, desipramine; *DAT*, dopamine transporter; *NET*, NE transporter.

expressed as the mean  $\pm$  S.E. Experiments with more than two groups were subjected to one-way ANOVA or two-way ANOVA followed by post hoc Tukey tests. Experiments with two groups were analyzed statistically using unpaired Student's *t* tests.

## RESULTS

**SNRIs Induce a Synergistic Reduction of AMPAR-mediated Synaptic Transmission in PFC Pyramidal Neurons**—To understand the interactive role of the 5-HT and NE systems in glutamatergic transmission, we recorded AMPAR-EPSC in PFC slices. Reuptake inhibitors fluoxetine and desipramine were used to elevate the synaptic concentration of endogenous 5-HT and NE, respectively. As shown in Fig. 1, *A* and *B*, bath application of fluoxetine (10  $\mu\text{M}$ ) or desipramine (10  $\mu\text{M}$ ) alone did not significantly alter AMPAR-EPSC (fluoxetine,  $7.2 \pm 1.7\%$ ,  $n = 5$ ;

desipramine,  $9.8 \pm 1.6\%$ ,  $n = 7$ ;  $p > 0.05$ , ANOVA). However, co-application of both inhibitors induced a substantial reduction of AMPAR-EPSC amplitude by  $48.8 \pm 4.9\%$  ( $n = 10$ ;  $p < 0.001$ , ANOVA). Dose-dependent experiments using fluoxetine and/or desipramine are shown in Fig. 1*C*. AMPAR-EPSC was not sensitive to either inhibitor at a dosage of less than 10  $\mu\text{M}$  but was significantly reduced by both inhibitors at low doses (5  $\mu\text{M}$ ,  $23.5 \pm 1.8\%$ ; 10  $\mu\text{M}$ ,  $49.0 \pm 3.9\%$ ;  $p < 0.001$ , ANOVA). Because the dual action of fluoxetine and desipramine at 10  $\mu\text{M}$  gave a saturating effect on AMPAR currents, we selected this concentration for the remaining experiments.

Next, we tested whether the synergistic reduction of AMPAR-EPSC by SNRIs also occurred *in vivo*. Animals were intraperitoneally injected with fluoxetine (5 mg/kg; 1 h) and/or desipramine (1 mg/kg; 1 h) before slicing and recording. As

## Modulation of AMPARs by 5-HT and NE Dual Reuptake Inhibitors

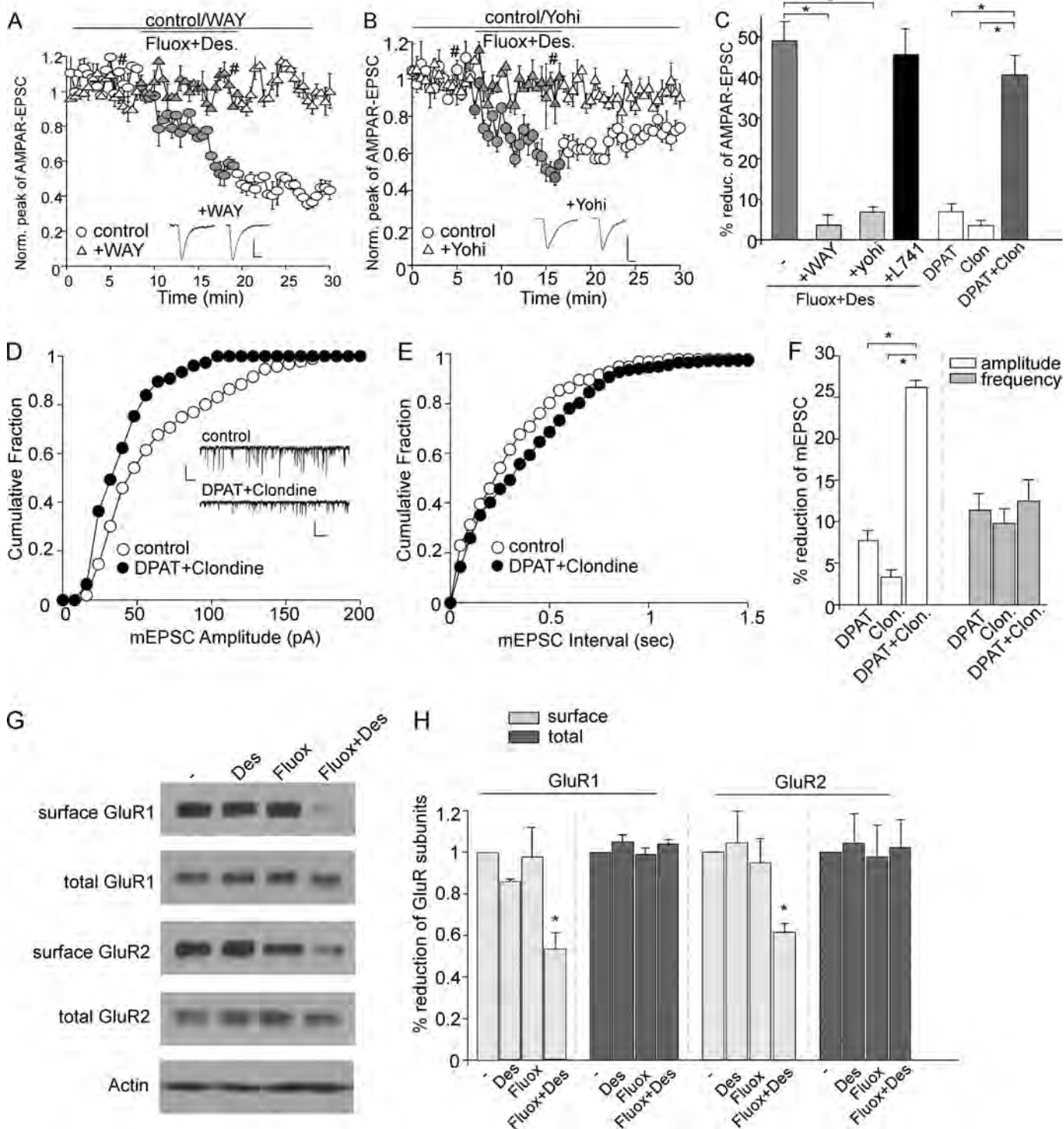


**FIGURE 2.** 5-HT<sub>1A</sub> and  $\alpha_2$ -AR co-activation mediates the regulation of AMPAR-EPSC and AMPAR surface expression by SNRIs. *A* and *B*, plot of normalized (Norm.) AMPAR-EPSC showing the effect of SNRIs in the presence of 5-HT<sub>1A</sub> antagonist WAY-100635 (WAY) (200 nM; *A*) or  $\alpha_2$ -AR antagonist yohimbine (Yohi) (40  $\mu$ M; *B*). *B*, representative current traces taken from the time points denoted by #. Scale bars, 50 pA, 10 ms. *C*, bar graph (mean  $\pm$  S.E.) showing the percentage of reduction (reduc.) of AMPAR-EPSCs by SNRIs in the presence of various pharmacological reagents affecting 5-HT, NE, or dopamine systems. L741, L741,742. \*,  $p < 0.01$ , one-way ANOVA. *D* and *E*, cumulative distribution of mEPSC amplitudes (*D*) or interevent intervals (*E*) in cultured PFC neurons co-treated with 8-OH-DPAT (DPAT) (5  $\mu$ M; 10 min) and clonidine (Clon) (5  $\mu$ M; 10 min). Scale bar, 100 pA, 10 ms. *F*, cumulative data (mean  $\pm$  S.E.) summarizing the percentage of reduction of mEPSC amplitude and frequency by 5-HT<sub>1A</sub> and  $\alpha_2$ -AR agonists. \*,  $p < 0.01$ , one-way ANOVA. *G* and *H*, Biotinylation assay showing the levels of surface GluR1 and GluR2 in PFC slices treated with fluoxetine (Fluox), desipramine (Des), or both (10  $\mu$ M; 10 min). \*,  $p < 0.01$ , one-way ANOVA. Error bars represent S.E.

shown in Fig. 1, *D* and *E*, AMPAR-EPSC was not altered in animals injected with fluoxetine or desipramine alone (saline,  $n = 12$ ; fluoxetine,  $n = 11$ ; desipramine,  $n = 10$ ) but was signif-

icantly reduced in those co-injected with desipramine and fluoxetine (desipramine + fluoxetine,  $n = 10$ ;  $F_{4,192} = 13.8$ ,  $p < 0.001$ , ANOVA). These data suggest that endogenous serotonin

and norepinephrine induce a synergistic down-regulation of glutamatergic transmission *in vivo*.

To test whether a *bona fide* SNRI has the same effect as fluoxetine plus desipramine, we examined venlafaxine, an SNRI used for treating certain anxiety disorders with depression. As shown in Fig. 1F, bath application of venlafaxine to cortical slices reduced AMPAR-EPSC in a dose-dependent manner with a significant effect at 50  $\mu\text{M}$  ( $25.5 \pm 4.2\%$ ;  $n = 5$ ;  $F_{3,16} = 11.2$ ,  $p < 0.001$ , ANOVA). PFC neurons from animals with an intraperitoneal injection of venlafaxine (8 mg/kg; 1 h) also showed a significant reduction of AMPAR-EPSC (saline,  $n = 10$ ; venlafaxine,  $n = 10$ ;  $F_{4,90} = 7.6$ ,  $p < 0.001$ , two-way ANOVA).

**Co-activation of 5-HT<sub>1A</sub> and  $\alpha_2$ -AR Receptors Mediates the Synergistic Reduction of AMPAR Currents and Surface Expression by SNRIs**—To determine which receptors underlie the synergistic regulation of AMPARs by SNRIs, we used specific receptor antagonists. As shown in Fig. 2, A–C, 5-HT<sub>1A</sub> antagonist WAY-100635 (200 nM) or  $\alpha_2$ -AR antagonist yohimbine (40  $\mu\text{M}$ ) alone completely blocked the synergistic reduction of AMPAR-EPSC by desipramine and fluoxetine (WAY-100635,  $3.1 \pm 2.8\%$ ,  $n = 5$ ; yohimbine,  $7.0 \pm 1.5\%$ ,  $n = 6$ ), suggesting that simultaneous activation of both receptors is required for the effect of SNRIs. However, dopamine D4 receptor antagonist L741,742 (10  $\mu\text{M}$ ) failed to alter the synergistic reduction of AMPAR-EPSC by desipramine and fluoxetine ( $45.6 \pm 6.3\%$ ;  $n = 5$ ), excluding the potential involvement of D4 receptors. Moreover, co-application of 5-HT<sub>1A</sub> agonist 8-OH-DPAT (5  $\mu\text{M}$ ) and  $\alpha_2$ -AR agonist clonidine (5  $\mu\text{M}$ ) significantly reduced AMPAR-EPSC ( $40.6 \pm 4.6\%$ ;  $n = 12$ ;  $p < 0.001$ , ANOVA), whereas neither of the single agonists was effective (8-OH-DPAT,  $7.0 \pm 1.9\%$ ,  $n = 8$ ; clonidine,  $3.6 \pm 1.9\%$ ,  $n = 5$ ;  $p > 0.05$ , ANOVA). Taken together, these results suggest that co-activation of 5-HT<sub>1A</sub> and  $\alpha_2$ -AR underlies the synergistic reduction of AMPAR currents by dual reuptake inhibitors.

Stimulation of serotonin and norepinephrine receptors may alter presynaptic glutamate release, which can contribute to the change in AMPAR-EPSC. To examine this possibility, we recorded mEPSC, which results from the random release of single transmitter vesicles. Significant changes in mEPSC amplitude reflect modifications of postsynaptic glutamate receptors. As shown in Fig. 2, D–F, co-application of 8-OH-DPAT (5  $\mu\text{M}$ ) and clonidine (5  $\mu\text{M}$ ) primarily reduced mEPSC amplitude ( $26.3 \pm 1.6\%$ ;  $n = 6$ ;  $p < 0.001$ , ANOVA) but not frequency ( $12.5 \pm 3.2\%$ ;  $n = 6$ ;  $p > 0.05$ , ANOVA). No significant reduction of mEPSC was observed with 8-OH-DPAT alone (amplitude,  $7.8 \pm 1.9\%$ ; frequency,  $11.4 \pm 2.4\%$ ;  $n = 7$ ;  $p > 0.05$ , ANOVA) or clonidine alone (amplitude,  $3.3 \pm 1.2\%$ ; frequency,  $9.8 \pm 2.0\%$ ;  $n = 6$ ;  $p > 0.05$ , ANOVA). Moreover, the paired pulse (interval, 0.1 s) ratio of AMPAR-EPSC (an index of presynaptic glutamate release) was unchanged in PFC slices treated with fluoxetine and desipramine (control,  $1.37 \pm 0.05$ ; fluoxetine + desipramine,  $1.4 \pm 0.04$ ;  $n = 4$ ;  $p > 0.05$ , ANOVA). These data suggest that the reduction of AMPAR-EPSC by 5-HT<sub>1A</sub> and  $\alpha_2$ -AR co-activation does not result from presynaptic changes.

We next examined the effect of SNRIs on AMPAR surface expression. As shown in Fig. 2, G and H, the level of surface

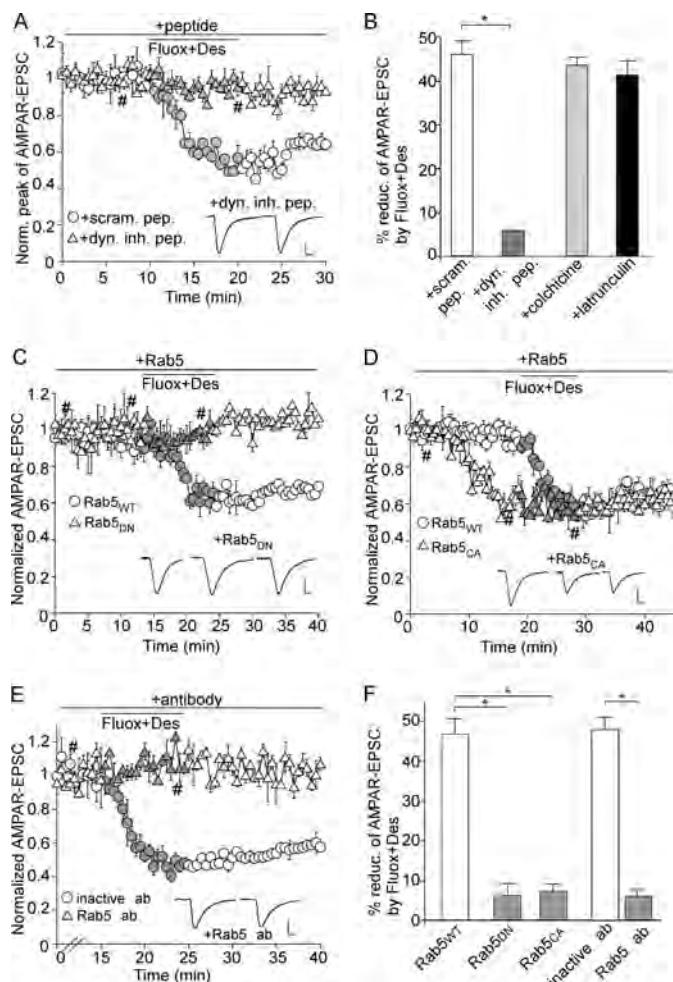


**FIGURE 3. Dynamin/Rab5-dependent AMPAR endocytosis underlies the effect of SNRIs on AMPAR-EPSC.** A, plot of normalized (Norm.) AMPAR-EPSC showing the effect of SNRIs in neurons injected with the dynamin inhibitory peptide (*dyn. inh. pep.*) (50  $\mu\text{M}$ ) versus a scrambled control peptide (*scram. pep.*). B, cumulative data (mean  $\pm$  S.E.) showing the effect of SNRIs on EPSC in neurons dialyzed with various reagents to perturb endocytosis or the cytoskeleton.  $*p < 0.01$ , one-way ANOVA. C–E, plots of normalized AMPAR-EPSC showing the effect of SNRIs in neurons injected with Rab5<sub>WT</sub> versus Rab5<sub>DN</sub> or Rab5<sub>CA</sub> proteins (all 4  $\mu\text{g}/\text{ml}$ ; C and D) or a Rab5 antibody (*Rab5 ab*) versus a heat-inactivated antibody (*inactive ab*) (2  $\mu\text{g}/\text{ml}$ ; E). Inset, representative current traces taken from the time points denoted by #. Scale bars, 50 pA, 10 ms. F, cumulative data (mean  $\pm$  S.E.) showing the effect of SNRIs on EPSC in neurons dialyzed with various reagents affecting Rab5 activity.  $*p < 0.01$ , one-way ANOVA. Error bars represent S.E. Fluox, fluoxetine; Des, desipramine; *reduc.*, reduction.

GluR1 and GluR2 subunits was significantly decreased in PFC slices co-treated with fluoxetine and desipramine (GluR1,  $0.53 \pm 0.08$  of control; GluR2,  $0.62 \pm 0.04$  of control;  $n = 4$ ;  $p < 0.001$ , ANOVA) but not with the application of fluoxetine alone (GluR1,  $0.98 \pm 0.15$  of control; GluR2,  $0.95 \pm 0.11$  of control;  $n = 4$ ;  $p > 0.05$ , ANOVA) or desipramine alone (GluR1,  $0.85 \pm 0.01$  of control; GluR2,  $1.04 \pm 0.16$  of control;  $n = 4$ ;  $p > 0.05$ , ANOVA). These data suggest that SNRIs might alter AMPAR-mediated synaptic responses by changing the surface expression of AMPARs.

**The Regulation of AMPARs by SNRIs Involves Dynamin/Rab5-dependent AMPAR Endocytosis**—Because SNRIs reduce surface AMPARs, we tested whether this results from increased internalization of surface AMPARs or from decreased AMPAR

## Modulation of AMPARs by 5-HT and NE Dual Reuptake Inhibitors

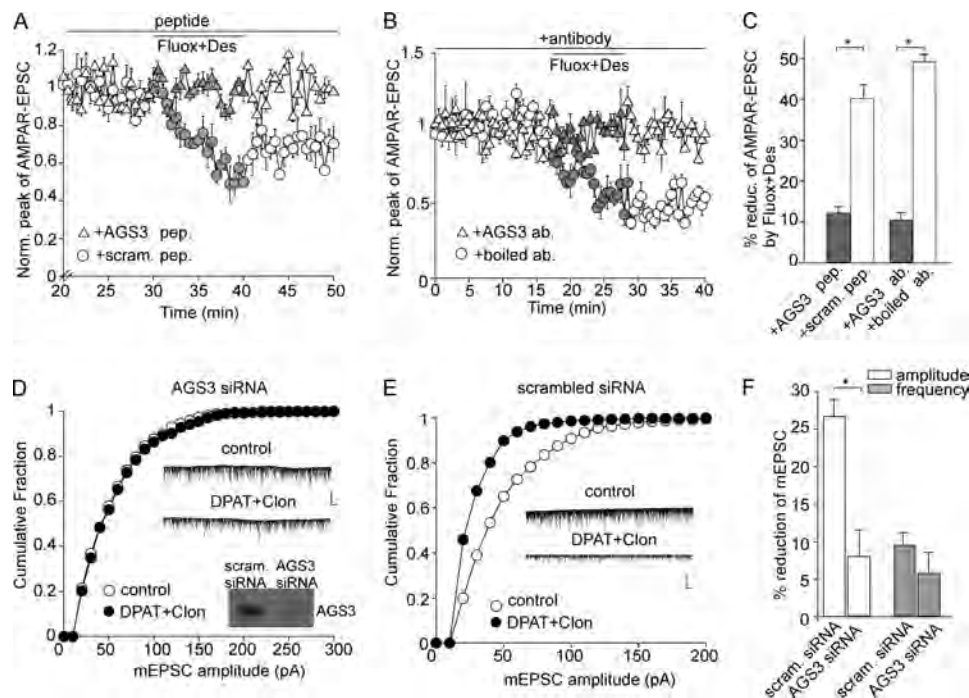


**FIGURE 4. AGS3, a G protein modulator, is involved in the synergistic regulation of AMPARs by SNRIs.** *A* and *B*, plot of normalized peak AMPAR-EPSC showing the effect of SNRIs in neurons dialyzed with AGS3 inhibitory peptide (*AGS3 pep.*) (50  $\mu$ M) versus a scrambled control peptide (*scram. pep.*) (*A*) or with anti-AGS3 (*AGS3 ab*) (4  $\mu$ g/ml) versus the heat-inactivated antibody (*boiled ab*) (*B*). *C*, cumulative data demonstrating the percentage of reduction of EPSC by SNRIs in the presence of various AGS3 inhibitors. \*,  $p < 0.01$ , *t* test. *D* and *E*, cumulative distribution of mEPSC amplitudes in the absence and presence of clonidine (*Clon*) plus 8-OH-DPAT (*DPAT*) in cultured PFC neurons transfected with AGS3 siRNA (*D*) versus a scrambled (*scram.*) control siRNA (*E*). *Inset* in *D*, Western blot showing the knockdown of AGS3 expression in AGS3 siRNA-transfected cortical cultures. *F*, summarized data showing the percentage of reduction of mEPSC amplitude and frequency by 8-OH-DPAT plus clonidine in neurons transfected with different siRNAs. \*,  $p < 0.01$ , *t* test. Error bars represent S.E. *Fluox*, fluoxetine; *Des*, desipramine.

transport along cytoskeletons. To do so, we dialyzed neurons with a dynamin inhibitory peptide (50  $\mu$ M) that disrupts amphiphysin-dynamin binding and thus prevents endocytosis through clathrin-coated pits (28). As shown in Fig. 3, *A* and *B*, the dynamin inhibitory peptide prevented the reduction of AMPAR-EPSCs by fluoxetine and desipramine ( $5.8 \pm 1.6\%$ ;  $n = 7$ ), whereas a scrambled control peptide was ineffective ( $46.0 \pm 3.3\%$ ;  $n = 6$ ). Dialysis of reagents that perturb microtubule or actin stability failed to alter the effect of SNRIs on AMPAR-EPSC (30  $\mu$ M colchicine,  $43.8 \pm 2.2\%$ ,  $n = 6$ ; 5  $\mu$ M latrunculin,  $41.0 \pm 3.2\%$ ,  $n = 6$ ; Fig. 3*B*), which ruled out the involvement of cytoskeleton-dependent transport of AMPARs. These data suggest that the regulation of AMPARs by SNRIs relies on dynamin-dependent AMPAR endocytosis.

A key player regulating vesicle transport between organelles in the exocytic/endocytic cycle is the Rab family of small GTPases (29). Rab5 has been suggested to control the transport of proteins from plasma membrane to early endosomes (30, 31). To examine whether SNRIs induce AMPAR endocytosis via Rab5, we infused cells with purified Rab5 proteins, including wild type (Rab5<sub>WT</sub>), dominant negative (Rab5<sub>DN</sub>), and catalytically active (Rab5<sub>CA</sub>). As shown in Fig. 3, *C–F*, fluoxetine plus desipramine lost the capability to reduce AMPAR-EPSC in Rab5<sub>DN</sub>-infused neurons ( $6.8 \pm 2.5\%$ ;  $n = 6$ ) but not in Rab5<sub>WT</sub>-injected cells ( $46.9 \pm 4.5\%$ ;  $n = 7$ ). Dialysis of Rab5<sub>CA</sub> alone caused a gradual decline of basal AMPAR-EPSC ( $41.5 \pm 4.3\%$ ;  $n = 5$ ) and occluded the subsequent effect of fluoxetine plus desipramine ( $7.5 \pm 2.1\%$ ;  $n = 5$ ). Moreover, inhibiting endogenous Rab5 function by injecting an antibody against

Rab5 blocked the effect of SNRIs on AMPAR-EPSC (Rab5 antibody,  $5.4 \pm 1.6\%$ ,  $n = 6$ ; heat-inactivated antibody,  $47.5 \pm 3.2\%$ ,  $n = 5$ ). Taken together, these findings suggest that the reduction of AMPAR synaptic responses by SNRIs involves the dynamin/Rab5-dependent endocytosis of AMPARs.

*AGS3, a G Protein Modulator, Is Involved in the Synergistic Regulation of AMPARs by SNRIs*—We next sought to examine the molecular mechanisms underlying the synergistic regulation of AMPARs by SNRIs. Both  $\alpha_2$ -AR and 5-HT<sub>1A</sub> are G<sub>i</sub>-coupled receptors. G-protein signaling is initiated with the dissociation of  $\beta\gamma$  and  $\alpha$  subunits and is terminated by reassociation of the two. AGS3 binds to  $\beta\gamma$  subunit and prevents it from reassociating with G<sub>i</sub>  $\alpha$  subunit, resulting in persistent activation of  $\beta\gamma$ -mediated signaling (32). To test whether AGS3 could be the key synergistic modulator in the regulation of AMPARs by SNRIs, we dialyzed neurons with a peptide derived from AGS3 (GRKKRRQRRRPPTMGEEFFDLLAKSQSKRMDD-QRVDLAK), which interrupts the AGS3- $\beta\gamma$  binding (33). As shown in Fig. 4, *A–C*, AGS3 peptide abolished the reduction of AMPAR-EPSC by co-application of fluoxetine and desipramine (AGS3 peptide,  $12.2 \pm 1.6\%$ ,  $n = 5$ ; control peptide,  $40.2 \pm 3.5\%$ ,  $n = 5$ ). Moreover, inhibiting intracellular AGS3 function by infusing an AGS3 antibody gave similar blockade (AGS3 antibody,  $10.8 \pm 1.8\%$ ,  $n = 6$ ; heat-inactivated antibody,  $49.3 \pm 1.9\%$ ,  $n = 5$ ).

To further test the involvement of AGS3, we utilized the siRNA approach to knock down AGS3. As shown in Fig. 4, *D–F*, AGS3 siRNA induced a significant suppression of AGS3 expression in cortical cultures. 8-OH-DPAT plus clonidine failed to

reduce mEPSC in AGS3 siRNA-transfected neurons (amplitude,  $8.0 \pm 3.4\%$ ; frequency,  $5.6 \pm 2.6\%$ ;  $n = 7$ ), but not in scrambled siRNA-transfected cells (amplitude,  $26.1 \pm 2.5\%$ ; frequency,  $9.3 \pm 1.6\%$ ;  $n = 6$ ). Taken together, these lines of evidence indicate that 5-HT<sub>1A</sub> and  $\alpha_2$ -AR synergistically down-regulate AMPAR-EPSC through a mechanism involving AGS3-facilitated G protein signaling.

**5-HT<sub>1A</sub> and  $\alpha_2$ -AR Receptors Synergistically Activate p38 Kinase in an AGS3-dependent Manner**—We further investigated the mechanism downstream of AGS3/G protein signaling that leads to the reduction of AMPAR-EPSC by SNRIs. A potential candidate is p38 MAPK, activation of which can induce the removal of synaptic AMPARs (34). To test this, we dialyzed neurons with p38 inhibitor SB203480 (20  $\mu$ M). The p44/42 MAPK inhibitor PD98059 (40  $\mu$ M) was used as a control. As shown in Fig. 5, A and B, fluoxetine and desipramine lost the capability to reduce AMPAR-EPSC significantly in the presence of SB203480 ( $11.0 \pm 1.7\%$ ;  $n = 6$ ) but not PD98059 ( $45.6 \pm 3.5\%$ ;  $n = 5$ ).

To examine whether co-stimulation of 5-HT<sub>1A</sub> and  $\alpha_2$ -AR receptors activates p38 MAPK via AGS3, we transfected neurons with AGS3 siRNA followed by measuring the level of active (Thr-180/Tyr-182 phosphorylated) p38 MAPK (35). As shown in Fig. 5, C and D, co-treatment with 8-OH-DPAT and clonidine increased p38 activity in neurons transfected with a control siRNA ( $2.1 \pm 0.15$  of control;  $n = 4$ ), and this effect was abolished in cells transfected with AGS3 siRNA ( $1.25 \pm 0.1$  of control;  $n = 4$ ). Application of 8-OH-DPAT or clonidine alone did not affect p38 activity. The activity of p44/42 was not altered by co-treatment with 8-OH-DPAT and clonidine. Consistent with the Western blotting results, immunocytochemical data (Fig. 5, E and F) showed that 8-OH-DPAT plus clonidine treatment increased the level of active p38 in cultured neurons transfected with a control siRNA (control,  $1 \pm 0.05$ ; 8-OH-DPAT + clonidine,  $1.87 \pm 0.05$ ;  $n = 19$ – $22$ ;  $p < 0.001$ , ANOVA) but not AGS3 siRNA (control,  $0.93 \pm 0.11$ ; 8-OH-DPAT + clonidine,  $0.83 \pm 0.05$ ;  $n = 19$ – $21$ ). Taken together, these results suggest that 5-HT<sub>1A</sub> and  $\alpha_2$ -AR receptor co-activation synergistically reduces AMPARs via AGS3-dependent activation of p38 MAPK.

## DISCUSSION

Monoamine hypofunction has long been proposed to underlie the pathophysiology of depression and anxiety disorders (6, 36). Data suggest that the interplay of NE with 5-HT may exert neurobiological normalization in mental illnesses (37). Dual enhancement of the NE and 5-HT systems produces better therapeutic outcome than targeting only one monoamine system (4, 8). The class of SNRIs now comprises three medications, venlafaxine, milnacipran, and duloxetine, all of which are efficacious in treating a variety of anxiety disorders and helpful in relieving chronic pain associated with and independent of depression (38). Evidence from meta-analysis of clinical trials supports the greater efficacy of venlafaxine and duloxetine in moderate to severe depression compared with selective serotonin reuptake inhibitors (9).

Using combined electrophysiological, biochemical, and immunocytochemical approaches, we found that application of

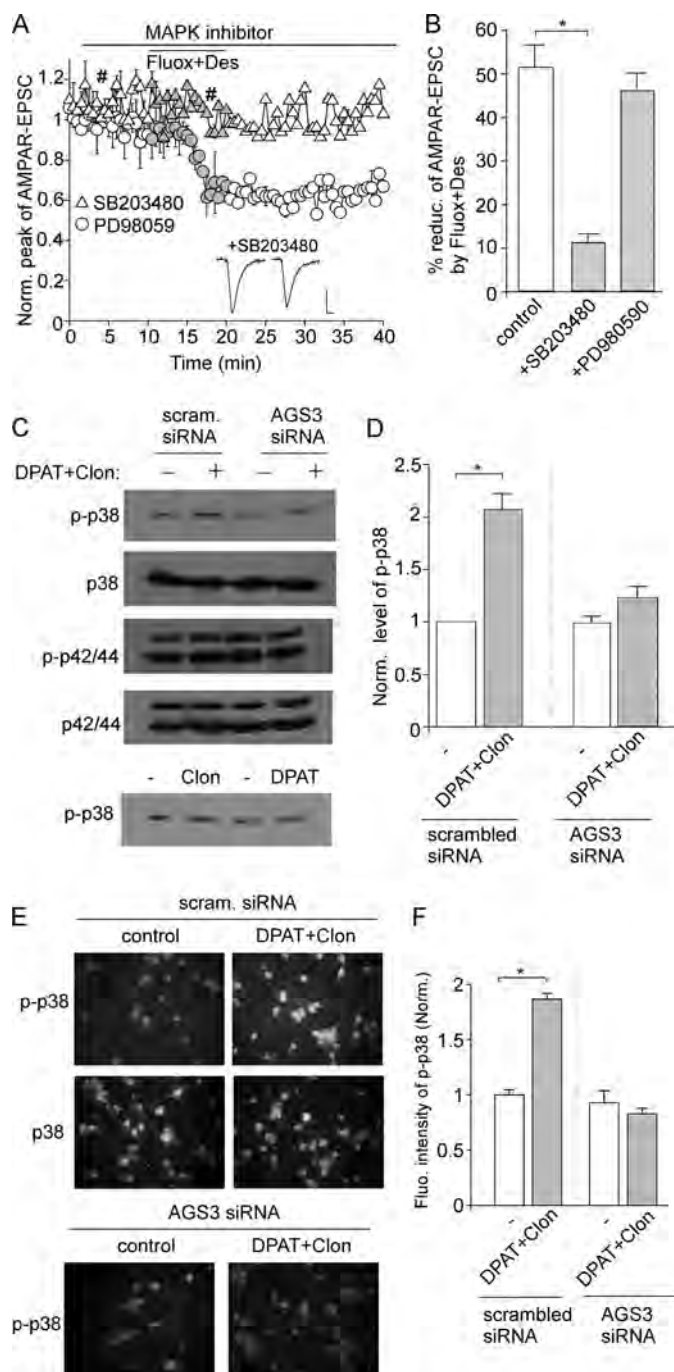


**FIGURE 5. The p38 MAPK is important for SNRI regulation of AMPARs, and it is synergistically activated by 5-HT<sub>1A</sub> and  $\alpha_2$ -AR receptors in an AGS3-dependent manner.** A, plot of normalized (*Norm.*) AMPAR-EPSCs showing the effect of SNRIs in neurons dialyzed with inhibitors for p38 (SB203480; 40  $\mu$ M) or p44/42 (PD98059; 40  $\mu$ M) MAPK. B, bar graphs summarizing the percentage of reduction (*reduc.*) of EPSCs by SNRIs in the presence of different MAPK inhibitors. \*,  $p < 0.01$ , one-way ANOVA. C and D, Western blots and quantifications showing the effect of 8-OH-DPAT (DPAT) and clonidine (*Clon*) (both 5  $\mu$ M; 10 min) on phospho-p38 (*p-p38*) or phospho-p42/44 (*p-p42/44*) MAPK (active) in cultured neurons transfected with AGS3 siRNA or a scrambled (*scram.*) control siRNA. \*,  $p < 0.01$ , *t* test. E and F, immunocytochemical images and quantifications showing the effect of 8-OH-DPAT and clonidine on total p38 and phospho-p38 levels in cultured neurons transfected with AGS3 siRNA or a scrambled control siRNA. \*,  $p < 0.01$ , *t* test. Error bars represent S.E. *Fluo.*, fluorescence; *Fluox*, fluoxetine; *Des*, desipramine.

low dose SNRI synergistically decreased AMPAR surface expression and function in PFC pyramidal neurons. Because high concentrations of single reuptake inhibitors are toxic and

## Modulation of AMPARs by 5-HT and NE Dual Reuptake Inhibitors

even lethal (39), our results suggest that using a low dose SNRI may provide more effective regulation of synaptic transmission in the prefrontal cortex, which is important for cognitive and emotional processes. Moreover, the SNRI-induced synergistic activation of signaling cascades to alter synaptic function may accelerate the onset of therapeutic effects.

Pharmacological evidence suggests that the synergistic regulation of AMPARs by SNRIs is mediated by 5-HT<sub>1A</sub> and  $\alpha_2$ -AR receptors, both of which are enriched at glutamatergic synapses (12, 13). An important player involved in the synergistic actions of  $\alpha_2$ -AR and 5-HT<sub>1A</sub> receptors is AGS3, which prolongs  $\beta\gamma$ -mediated signaling by preventing the reassociation of G<sub>i</sub>  $\alpha$  subunit (32). Consistent with this finding, AGS3 also mediates the synergy between  $\mu$ -opioid and cannabinoid CB1 receptors (40).

Co-stimulation of 5-HT<sub>1A</sub> and  $\alpha_2$ -AR receptors induces AGS3-dependent activation of p38 MAPK, probably via G protein  $\beta\gamma$  subunit, small GTPase Rap1, and MAPK kinases 3/6, similarly to metabotropic glutamate receptors (41). Activation of p38 MAPK was found to be required for the removal of synaptic AMPARs and synaptic depression (34). Our previous study has also shown that G protein-coupled receptors, such as metabotropic glutamate receptors, could induce the activation of p38 MAPK, leading to Rab5-mediated AMPAR endocytosis and long term depression in PFC neurons (42). Here, we have demonstrated that p38 MAPK is the key molecule responsible for SNRI reduction of AMPAR-EPSC. p38 MAPK was found to modulate endocytic trafficking by regulating the functional cycle of Rab5 between the membrane and cytosol that is controlled by guanyl nucleotide dissociation inhibitor (43). Thus, SNRI activation of p38 MAPK may accelerate AMPAR endocytosis by stimulating the formation of Rab5-guanyl nucleotide dissociation inhibitor complex. Another possibility is that the SNRI alters AMPAR recycling because some AMPA receptors undergo constitutive endocytic recycling, and dynamin and Rab5 blockade could impact receptor recycling directly. Taken together, our study has revealed the synergistic regulation of PFC glutamatergic transmission by co-activation of the serotonin and norepinephrine systems, providing a potential basis for the better therapeutic effects of dual reuptake inhibitors in the treatment of mental disorders.

*Acknowledgment*—We thank Xiaoqing Chen for technical support.

### REFERENCES

1. Arnsten, A. F., and Li, B. M. (2005) Neurobiology of executive functions: catecholamine influences on prefrontal cortical functions. *Biol. Psychiatry* **57**, 1377–1384
2. Cools, R., Roberts, A. C., and Robbins, T. W. (2008) Serotonergic regulation of emotional and behavioural control processes. *Trends Cogn. Sci.* **12**, 31–40
3. Ninan, P. T. (1999) The functional anatomy, neurochemistry, and pharmacology of anxiety. *J. Clin. Psychiatry* **60**, Suppl. 22, 12–17
4. Tran, P. V., Bymaster, F. P., McNamara, R. K., and Potter, W. Z. (2003) Dual monoamine modulation for improved treatment of major depressive disorder. *J. Clin. Psychopharmacol.* **23**, 78–86
5. Jobe, P. C., and Browning, R. A. (2005) The serotonergic and noradrenergic effects of antidepressant drugs are anticonvulsant, not proconvulsant. *Epilepsy Behav.* **7**, 602–619

6. Kurian, M. A., Gissen, P., Smith, M., Heales, S., Jr., and Clayton, P. T. (2011) The monoamine neurotransmitter disorders: an expanding range of neurological syndromes. *Lancet Neurol.* **10**, 721–733
7. Crupi, R., Marino, A., and Cuzzocrea, S. (2011) New therapeutic strategy for mood disorders. *Curr. Med. Chem.* **18**, 4284–4298
8. Posternak, M. A., and Zimmerman, M. (2005) Dual reuptake inhibitors incur lower rates of tachyphylaxis than selective serotonin reuptake inhibitors: a retrospective study. *J. Clin. Psychiatry* **66**, 705–707
9. Bradley, A. J., and Lenox-Smith, A. J. (2013) Does adding noradrenergic reuptake inhibition to selective serotonin reuptake inhibition improve efficacy in patients with depression? A systematic review of meta-analyses and large randomised pragmatic trials. *J. Psychopharmacol.* **27**, 740–758
10. Andrade, R. (1998) Regulation of membrane excitability in the central nervous system by serotonin receptor subtypes. *Ann. N.Y. Acad. Sci.* **861**, 190–203
11. Ramos, B. P., and Arnsten, A. F. (2007) Adrenergic pharmacology and cognition: focus on the prefrontal cortex. *Pharmacol. Ther.* **113**, 523–536
12. Kia, H. K., Miquel, M. C., Brisorgueil, M. J., Daval, G., Riad, M., El Mestikawy, S., Hamon, M., and Vergé, D. (1996) Immunocytochemical localization of serotonin 1A receptors in the rat central nervous system. *J. Comp. Neurol.* **365**, 289–305
13. Wang, M., Ramos, B. P., Paspalas, C. D., Shu, Y., Simen, A., Duque, A., Vijayraghavan, S., Brennan, A., Dudley, A., Nou, E., Mazer, J. A., McCormick, D. A., and Arnsten, A. F. (2007)  $\alpha_2A$ -Adrenoceptors strengthen working memory networks by inhibiting cAMP-HCN channel signaling in prefrontal cortex. *Cell* **129**, 397–410
14. Heisler, L. K., Chu, H. M., Brennan, T. J., Danao, J. A., Bajwa, P., Parsons, L. H., and Tecott, L. H. (1998) Elevated anxiety and antidepressant-like responses in serotonin 5-HT<sub>1A</sub> receptor mutant mice. *Proc. Natl. Acad. Sci. U.S.A.* **95**, 15049–15054
15. Schramm, N. L., McDonald, M. P., and Limbird, L. E. (2001) The  $\alpha_{2a}$ -adrenergic receptor plays a protective role in mouse behavioral models of depression and anxiety. *J. Neurosci.* **21**, 4875–4882
16. Drevets, W. C., Frank, E., Price, J. C., Kupfer, D. J., Holt, D., Greer, P. J., Huang, Y., Gautier, C., and Mathis, C. (1999) PET imaging of serotonin 1A receptor binding in depression. *Biol. Psychiatry* **46**, 1375–1387
17. Escibá, P. V., Ozaita, A., and García-Sevilla, J. A. (2004) Increased mRNA expression of  $\alpha_2A$ -adrenoceptors, serotonin receptors and  $\mu$ -opioid receptors in the brains of suicide victims. *Neuropsychopharmacology* **29**, 1512–1521
18. Lemonde, S., Turecki, G., Bakish, D., Du, L., Hrdina, P. D., Bown, C. D., Sequeira, A., Kushwaha, N., Morris, S. J., Basak, A., Ou, X. M., and Albert, P. R. (2003) Impaired repression at a 5-hydroxytryptamine 1A receptor gene polymorphism associated with major depression and suicide. *J. Neurosci.* **23**, 8788–8799
19. Rausch, J. L., Johnson, M. E., Kasik, K. E., and Stahl, S. M. (2006) Temperature regulation in depression: functional 5HT<sub>1A</sub> receptor adaptation differentiates antidepressant response. *Neuropsychopharmacology* **31**, 2274–2280
20. Wakeno, M., Kato, M., Okugawa, G., Fukuda, T., Hosoi, Y., Takekita, Y., Yamashita, M., Nonen, S., Azuma, J., and Kinoshita, T. (2008) The  $\alpha_2A$ -adrenergic receptor gene polymorphism modifies antidepressant responses to milnacipran. *J. Clin. Psychopharmacol.* **28**, 518–524
21. Goldman-Rakic, P. S. (1995) Cellular basis of working memory. *Neuron* **14**, 477–485
22. Popoli, M., Yan, Z., McEwen, B. S., and Sanacora, G. (2012) The stressed synapse: the impact of stress and glucocorticoids on glutamate transmission. *Nat. Rev. Neurosci.* **13**, 22–37
23. Yuen, E. Y., Gu, Z., and Yan, Z. (2007) Calcineurin regulation of AMPA receptor channels in cortical pyramidal neurons. *J. Physiol.* **580**, 241–254
24. Yuen, E. Y., Wei, J., Liu, W., Zhong, P., Li, X., and Yan, Z. (2012) Repeated stress causes cognitive impairment by suppressing glutamate receptor expression and function in prefrontal cortex. *Neuron* **73**, 962–977
25. Yuen, E. Y., and Yan, Z. (2009) Dopamine D4 receptors regulate AMPA receptor trafficking and glutamatergic transmission in GABAergic interneurons of prefrontal cortex. *J. Neurosci.* **29**, 550–562
26. Yuen, E. Y., Jiang, Q., Chen, P., Feng, J., and Yan, Z. (2008) Activation of 5-HT<sub>2A/C</sub> receptors counteracts 5-HT<sub>1A</sub> regulation of *N*-methyl-D-as-

- partate receptor channels in pyramidal neurons of prefrontal cortex. *J. Biol. Chem.* **283**, 17194–17204
27. Chen, P., Gu, Z., Liu, W., and Yan, Z. (2007) Glycogen synthase kinase 3 regulates N-methyl-D-aspartate receptor channel trafficking and function in cortical neurons. *Mol. Pharmacol.* **72**, 40–51
  28. Gout, I., Dhand, R., Hiles, I. D., Fry, M. J., Panayotou, G., Das, P., Truong, O., Totty, N. F., Hsuan, J., and Booker, G. W. (1993) The GTPase dynamin binds to and is activated by a subset of SH3 domains. *Cell* **75**, 25–36
  29. Zerial, M., and McBride, H. (2001) Rab proteins as membrane organizers. *Nat. Rev. Mol. Cell Biol.* **2**, 107–117
  30. Bucci, C., Parton, R. G., Mather, I. H., Stunnenberg, H., Simons, K., Hofflack, B., and Zerial, M. (1992) The small GTPase rab5 functions as a regulatory factor in the early endocytic pathway. *Cell* **70**, 715–728
  31. Brown, T. C., Tran, I. C., Backos, D. S., and Esteban, J. A. (2005) NMDA receptor-dependent activation of the small GTPase Rab5 drives the removal of synaptic AMPA receptors during hippocampal LTD. *Neuron* **45**, 81–94
  32. Bernard, M. L., Peterson, Y. K., Chung, P., Jourdan, J., and Lanier, S. M. (2001) Selective interaction of AGS3 with G-proteins and the influence of AGS3 on the activation state of G-proteins. *J. Biol. Chem.* **276**, 1585–1593
  33. Bowers, M. S., McFarland, K., Lake, R. W., Peterson, Y. K., Lapish, C. C., Gregory, M. L., Lanier, S. M., and Kalivas, P. W. (2004) Activator of G protein signaling 3: a gatekeeper of cocaine sensitization and drug seeking. *Neuron* **42**, 269–281
  34. Zhu, J. J., Qin, Y., Zhao, M., Van Aelst, L., and Malinow, R. (2002) Ras and Rap control AMPA receptor trafficking during synaptic plasticity. *Cell* **110**, 443–455
  35. Han, J., Lee, J. D., Bibbs, L., and Ulevitch, R. J. (1994) A MAP kinase targeted by endotoxin and hyperosmolarity in mammalian cells. *Science* **265**, 808–811
  36. Nutt, D. J. (2002) The neuropharmacology of serotonin and noradrenaline in depression. *Int. Clin. Psychopharmacol.* **17**, Suppl. 1, S1–S12
  37. Goddard, A. W., Ball, S. G., Martinez, J., Robinson, M. J., Yang, C. R., Russell, J. M., and Shekhar, A. (2010) Current perspectives of the roles of the central norepinephrine system in anxiety and depression. *Depress. Anxiety* **27**, 339–350
  38. Stahl, S. M., Grady, M. M., Moret, C., and Briley, M. (2005) SNRIs: their pharmacology, clinical efficacy, and tolerability in comparison with other classes of antidepressants. *CNS Spectr.* **10**, 732–747
  39. Boyer, E. W., and Shannon, M. (2005) The serotonin syndrome. *N. Engl. J. Med.* **352**, 1112–1120
  40. Yao, L., McFarland, K., Fan, P., Jiang, Z., Ueda, T., and Diamond, I. (2006) Adenosine A2a blockade prevents synergy between mu-opiate and cannabinoid CB1 receptors and eliminates heroin-seeking behavior in addicted rats. *Proc. Natl. Acad. Sci. U.S.A.* **103**, 7877–7882
  41. Huang, C. C., You, J. L., Wu, M. Y., and Hsu, K. S. (2004) Rap1-induced p38 mitogen-activated protein kinase activation facilitates AMPA receptor trafficking via the GDI-Rab5 complex. Potential role in (S)-3,5-dihydroxyphenylglycine-induced long term depression. *J. Biol. Chem.* **279**, 12286–12292
  42. Zhong, P., Liu, W., Gu, Z., and Yan, Z. (2008) Serotonin facilitates long-term depression induction in prefrontal cortex via p38 MAPK/Rab5-mediated enhancement of AMPA receptor internalization. *J. Physiol.* **586**, 4465–4479
  43. Cavalli, V., Vilbois, F., Corti, M., Marcote, M. J., Tamura, K., Karin, M., Arkininstall, S., and Gruenberg, J. (2001) The stress-induced MAP kinase p38 regulates endocytic trafficking via the GDI:Rab5 complex. *Mol. Cell* **7**, 421–432